Experimental Setup for the Study of Air Leakage Patterns

Guylaine Desmarais **Dominique Derome** **Paul Fazio, Ph.D., P.E.**

ABSTRACT

A research project has been conducted to investigate the impact of the initial air leakage characteristics on the hygrothermal performance of insulated walls retrofitted with rigid insulation added either on the warm side or on the cold side of the wood studs. This paper presents the experimental setup developed to study and document the air leakage patterns.
The research project involves the construction of a test hut inside an environmental chamber where winter, and then spring, steady-state conditions are simulated. The methods used to assess the impact of the air leakage characteristics are the three-dimensional monitoring of temperatures and the two-dimensional monitoring of moisture contents within the assemblies. Temperature monitoring results are presented using isotherms for the assemblies with no rigid insulation added.

INTRODUCTION

Increased levels of insulation are being promoted to reduce energy consumption. In fact, different programs are currently being proposed by government agencies in Quebec and Canada to encourage and assist homeowners to add insulation to existing residential low-rise buildings.

One reason for this is that it is relatively easy to calculate the impact on energy consumption of thermal resistance added to the envelope. However, those heat transfer calculations typically do not take into account the potential for condensation due to moisture and air movement. Adding thermal resistance to exterior wall assemblies modifies their temperature gradient, and the risk for moisture accumulation and condensation may increase, especially if warm, moist indoor air is allowed to flow through them. Moisture may then accumulate in the wood and the insulation, inducing decay, mold growth, and the reduction of the thermal performance of the insulation.

Moisture from indoors can move through the wall by diffusion or exfiltration. Of the two, exfiltration is the main moisture transfer vehicle (Kumaran 1996) and, thus, an important cause of moisture-related problems. Most air exfiltrates through paths created by cracks, joints between materials, or junctions between assemblies; the latter are often the weak points of the assembly and are critical because of their potential for becoming concentrated areas of deterioration. Furthermore, "it has been demonstrated that walls with point defects on the warm side of the assembly showed moisture accumulation directly opposite the defect on the cold side when tested" (Forest 1989). Such paths that allow the flow of air are present in most existing exterior walls. To avoid problems, the initial air leakage characteristics of the envelope should therefore be taken into account when increasing the R-value of existing exterior wall assemblies. A more detailed knowledge of the flow of warm, moist air through the envelope is required in order to better ascertain the moisture-related risks taken by increasing the R-value of existing exterior wall assemblies.

Experiments including heat, air, and moisture transfer have already been conducted in laboratory settings on various exterior wall assemblies. They are used as a basis for the establishment of the experimental protocol for the present research project. The assemblies studied were wood frame exterior wall assemblies. The samples varied in size and were sandwiched between a cold and a hot chamber. Ojanen and Simonson (1995) also studied a wall junction and a wall/roof junction. Those assemblies were investigated with different insulation strategies, and/or different exterior sheathing, and/or different vapor barriers. The impact of air barriers was also studied by Ojanen and Kohonen (1995) and Trechsel et al. (1985, 1986). In some of the experiments, moisture was introduced directly into the assemblies (Ojanen and Kohonen 1995) to study their mode of drying. In others, interior air was

Guylaine Desmarais is a registered architect and a graduate student, **Dominique Derome** is a registered architect and a lecturer, and **Paul Fazio** is a professor in the School for Building, Concordia University, Montreal, Quebec, Canada.

allowed to flow through the wall assemblies. For example, Trechsel et al. (1986) made holes in the interior finish (two at the top and two at the bottom) at the beginning of the test, while in another experiment, Simpson and O'Connor (1994) added holes midway through the experiment. In both cases, the openings did not represent any specific air leakage path. In their experiment, Trechsel et al. (1986) also provided holes that could be sealed hermetically to allow the introduction of tracer gas in order to determine the direction of airflow in the cavity.

In this research project, the impact of different types of air leakage on the hygrothermal performance of walls with added rigid insulation either on the warm side or on the cold side of the wood studs is being monitored experimentally. The objective of this paper is to present the experimental setup developed to study specific air leakage patterns.

The procedure involves the construction of a full-scale test hut inside the environmental chamber where conditions representing Montreal winter and late spring weather are simulated. A previous research project conducted in the test hut mode demonstrated the feasibility of large-scale testing in the environmental chamber facility (Fazio et al. 1998). Two reinsulation strategies are studied, each with three different air leakage patterns, and compared to an insulated base case. The construction of the hut is typical of Quebec low-rise, wood frame residences insulated with fiberglass batt insulation between the studs. The methods implemented to assess the impact of air flowing through the assemblies include two-dimensional grid moisture monitoring and three-dimensional grid temperature monitoring.

EXPERIMENTAL PROCEDURE

Experimental Facility

The environmental chamber is a versatile research facility where the overall hygrothermal performance of exterior walls (with or without doors and windows) and/or roofs can be evaluated. It has been designed to meet the requirements for the guarded hot box standard test method (ASTM C 236-89). For this test, the facility is used in the environmental chamber mode. A complete description of the facility is found in Fazio et al. (1997).

The installation is composed of the following:

- The *cold box*, 24 ft, 6 in. (7.5 m) high by 14 ft, 5 in. (4.4 m) wide by 11 ft 10 in. (3.6 m) deep, in which temperatures ranging from –40°F (–40°C) to 120°F (40°C) can be maintained. The conditions are produced using a 5 ton screw compressor, a 12,000 cfm recirculation fan, and a 25 kW reheating heater. This box cannot be moved from its position. Its walls are made of 6 in. (150 mm) foamed polyurethane boards, laminated between 1/16 in. (1 mm) aluminum sheets on the outside and 1 mm stainless steel sheets on the inside.
- The *hot box*, 24 ft, 6 in. (7.5 m) high by 14 ft, 5 in. (4.4 m) wide by 19 ft, 8 in. (6 m) deep, heated with a 20 kW heater and cooled with a 1 ton cooling unit. Temperatures from 40°F (5°C) to 120°F (50°C) can be obtained. It is also equipped with a 600 cfm air recirculation system, a fresh air supply/return damper, and a humidification system. The hot box is movable toward and away from the cold box on four compressed air pads. Its walls are made of 6 in. (150 mm) foamed polyurethane boards, laminated between 1/16 in. (1 mm) aluminum sheets on the outside and 1/16 in. (1 mm) stainless steel sheets on the inside.
- The *data acquisition system.* It has 400 input channels, 10 output channels, 16 digital I/O channels, 8 solid-state relays, and 8 counter/timer channels. Readings are taken automatically every ten minutes for each measurement point.

The cold and hot boxes are joined forming a 24 ft, 6 in. (7.5 m) high by 14 ft, 5 in. (4.4 m) wide by 31 ft, 6 in. (9.6 m) deep climatic chamber, where full-scale test huts can be tested. Figure 1 illustrates the main parts of the environmental chamber facility, of which the specimen frame and the metering box are not used for this test.

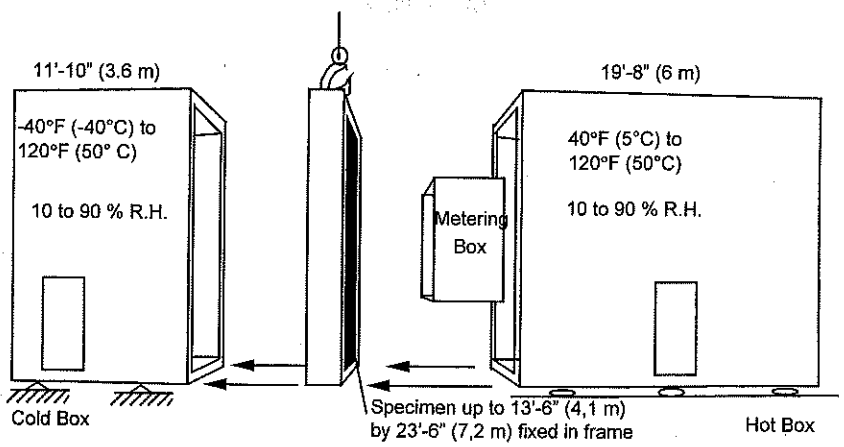

Figure 1 *Environmental chamber facility.*

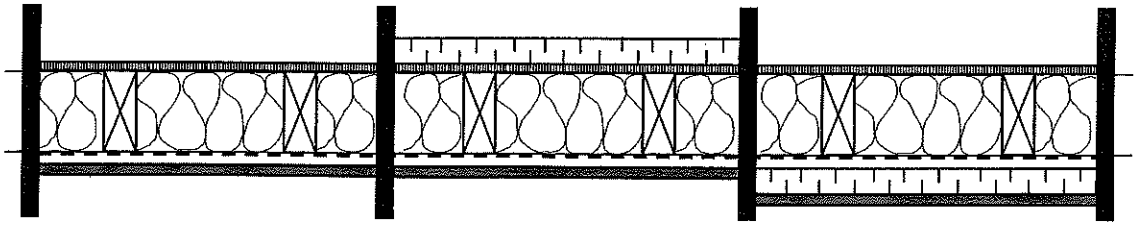

1. Base case

2. Rigid insulation added on the cold side of the studs.

3. Rigid insulation added on the warm side of the studs

Figure 2 *Compositions of the assemblies.*

Experimental Setup

A 13 ft, 9 in. (4.2 m) long by 8 ft, 4 in. (2.5 m) wide by 9 ft, 10 in. (3 m) high test hut has been built inside the environmental chamber. It models the second story of a house, which would normally be subjected to exfiltration during the winter months due to the stack effect. The test hut is exposed to simulated winter, and then spring, climatic conditions. Weather data collected for Montreal over 12 years are used to determine the actual conditions in the chamber and the test hut. The baseboard heater and the dehumidifier that provide the conditions inside the test hut are located in a box in its center. The air is mixed inside this box before circulating in the hut, ensuring more uniform conditions for all sample sections. The installation of the wall-mounted air-conditioning unit and the passage of the electrical and sensor wires are concentrated in one section between two studs where no monitoring is performed.

Three different exterior wall compositions, each representing a different insulation strategy, are studied. Three different patterns of air leakage are applied to those exterior wall compositions. In total, nine exterior wall sample sections are studied. Figure 2 illustrates the three compositions used for the project.

Test Specimens. In total, nine sample sections, 2 ft, 8 in. (0.8 m) wide by 8 ft, 0 in. (2.4 m) high, are being investigated. A sample section was defined as one 16 in. (360 mm) cavity flanked on each side by a nominal 2 in. by 4 in. (38 mm by 89 mm) stud and an 8 in. (180 mm) cavity. Each sample section is completely insulated according to the insulation strategy being investigated, and monitoring is performed only in the 16 in. (360 mm) central portion. The two half-cavities act as insulated "buffers" between the sample section and the adjacent ones. The sample sections are separated by oriented strand board (OSB) panels, 5/8 in. (16 mm) thick by 12 in. (300 mm) wide, painted with two coats of a special vapor barrier paint to prevent air and moisture transfer between the sample sections. The panels are wider than the assemblies to allow caulking of the finishes against the separators. They are sealed to the bottom and top plates. Figure 3 shows the wood structure and the separators.

Composition of the Assemblies. The composition of the walls (platform frame system with nominal 2 in. by 4 in. [38 mm by 89 mm] wood studs) is typical of single-family residential construction in Quebec. Statistics from the Association Provinciale des Constructeurs d'Habitations du Québec (APCHQ) were used to select the construction materials.

The junction between the exterior walls and the roof is built using common on-site techniques and materials. The setup simulates typical ventilated roofs. Even though it is not directly monitored, the junction of the roof is included in the overall hygrothermal behavior of the specimens. The composition of the roof, from outside to inside, is

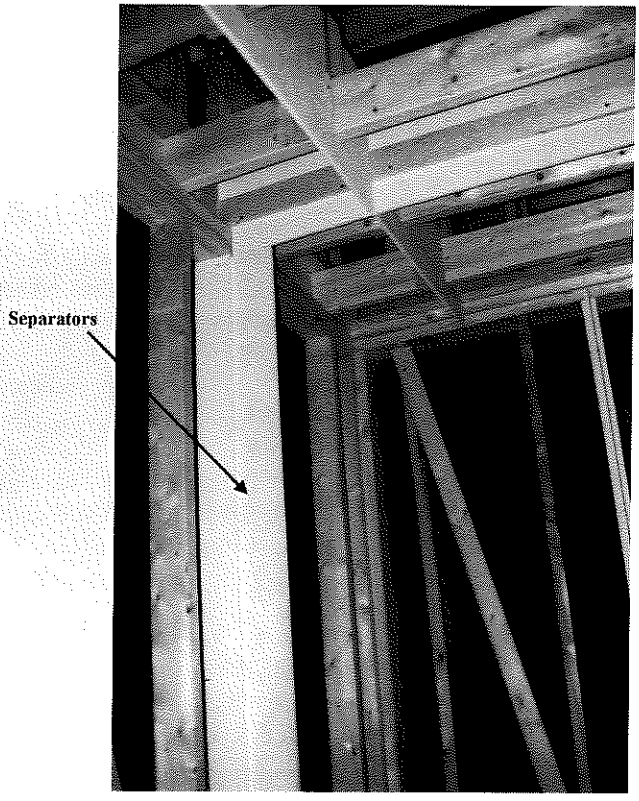

Figure 3 *Test hut wood structure and OSB separators.*

- ½ in. (13 mm) plywood;
- nominal 2 in. by 6 in. (38 mm by 140 mm) wood joists at 16 in. (400 mm) oc;
- 10 in. (250 mm) air space (ventilated to outside);
- nominal 2 in. by 6 in. (38 mm by 140 mm) wood joists at 16 in. (400 mm) oc;
- 10 in. (250 mm) of fiberglass batt insulation;
- nominal 1 in. by 3 in. (19 mm by 64 mm) wood furring at 16 in. (400 mm) oc;
- ½ in. (13 mm) gypsum board;
- standard latex paint (two coats).

The composition of the base case wall, from outside to inside, is

- spunbonded polyolefin membrane weather barrier;
- 3/8 in. (10 mm) asphalt impregnated fiberboard;
- nominal 2 in. by 4 in. (38 mm by 89 mm) wood studs at 16 in. (400 mm) oc;
- 3½ in. (89 mm) fiberglass batt insulation between the studs;
- 6 mil polyethylene membrane vapor barrier;
- nominal 1 in. by 3 in. (19 mm by 64 mm) horizontal wood furring at 16 in. (400 mm) oc;
- ½ in. (13 mm) gypsum board;
- standard latex paint (two coats).

For two sample sections, rigid extruded polystyrene insulation 1½ in. (38 mm) thick is added on the interior side, on the warm side of the vapor barrier. This method would be used if interior renovations are being performed and removal of the existing interior finish is necessary. The vapor barrier can be evaluated and repaired or replaced if necessary and airtightness can be improved from the inside.

For three sample sections, rigid extruded polystyrene insulation 1½ in. (38 mm) thick is added on the exterior side, directly on the existing fiberboard sheathing. This method, which requires the removal of the exterior veneer, would be used if the veneer needs to be replaced. Airtightness can then be improved from the outside.

If both the interior and exterior finishes appear to be in good condition, either of these two reinsulation strategies could be used to increase the thermal resistance of the wall. Figure 4 shows sample sections with rigid insulation added on the inside before installation of the interior finish and with rigid insulation added on the outside before installation of the spunbonded polyolefin.

Air Leakage Characteristics. The exterior wall compositions described above are studied with different air leakage characteristics. Many different types of air leakage paths can exist in exterior wall assemblies. Three are studied here:

- *Long air exfiltration path.* The air flows into the wall through a 1/16 in. (2 mm) horizontal crack at the bottom of the interior finish and out through a 3/16 in. (5 mm) horizontal crack at the top of the exterior sheathing, just below the top plate. This is the case if the gap between the interior finish and the floor is not sealed properly.
- *Direct air exfiltration path.* The air flows into the wall through a 13/16 in. (20 mm) diameter opening in the interior finish, centered between the studs and 12 in. (300 mm) above the floor. This might occur when air exits through an electrical outlet.
- *Diffuse exfiltration path.* The air flows into the wall uniformly through 42 holes, 1/8 in. (3 mm) in diameter

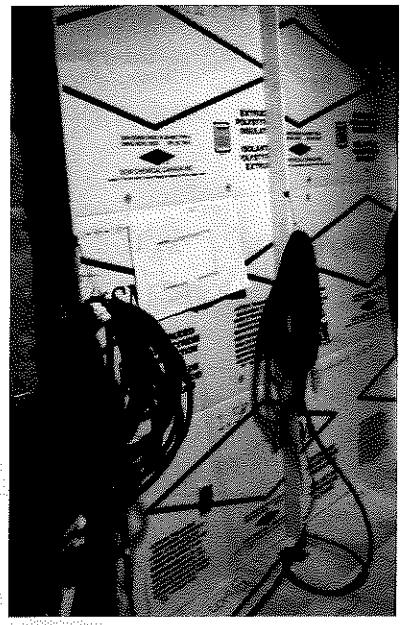

(a) Insulation added on the warm side of the wood studs.

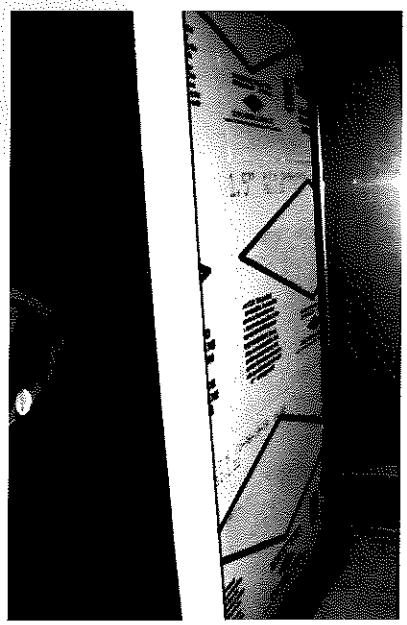

(b) Insulation added on the cold side of the wood studs.

Figure 4 *Sample sections with added rigid insulation.*

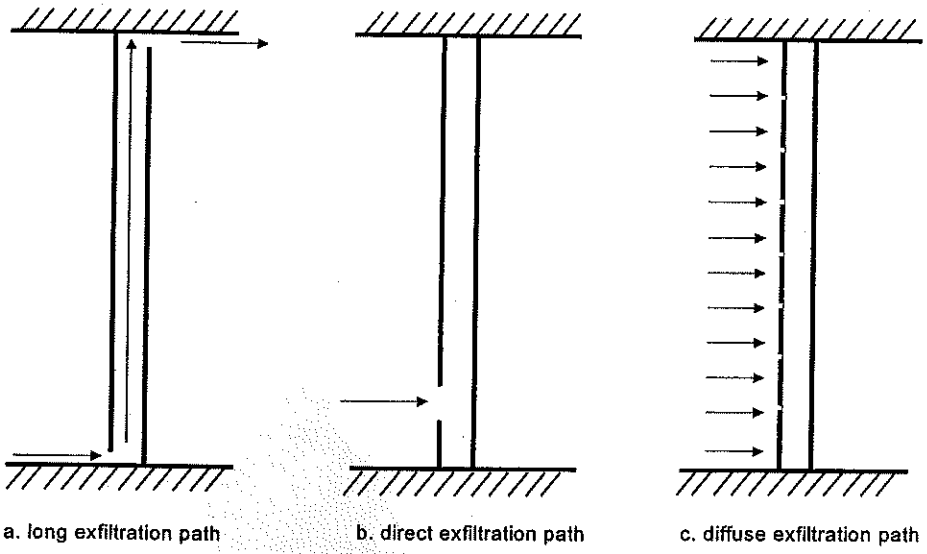

Figure 5 *Air leakage paths.*

(according to a 6 in. (150 mm) center-to-center grid), drilled in the interior finish, and out through the fiberboard sheathing. There are no holes through the fiberboard sheathing. Although it is not likely to occur in buildings using the usual construction materials (which have a certain airtightness), this type of flow is included because some simulation models take into account airflow only when it is uniform through the assembly.

The size of the openings is calculated so that the total area of openings in the interior finish is the same for the three air exfiltration paths. To serve as a reference, one base case section is sealed so that as little air as possible flows through it. Figure 5 illustrates the air leakage paths.

TABLE 1
Parameters of Sample Sections Tested

Sample Section ID	89 mm Fiberglass	38 mm Polystyrene Added Inside	38 mm Polystyrene Added Outside	Long Air Path	Direct Air Path	Diffuse Air Path	Airtight
1	■			■			
2	■				■		
3	■					■	
4	■		■	■			
5	■		■		■		
6	■		■			■	
7	■	■		■			
8	■	■			■		
9	■						■

Climatic Conditions. To study moisture accumulation and evacuation, the experiment is divided into two distinct climatic periods: one wetting period and one drying period. Actual average daily temperatures for Montreal from January 1986 to November 1997 are used to get average monthly temperatures. Those are then compiled to get an overall average temperature for each month of the year. Those overall monthly averages are used to determine the coldest weather of the year for the wetting period and the late spring conditions for the drying period.

In previous experiments, the duration of the exposure to wetting climatic conditions has varied from 5 days (Trechsel et al. 1985, 1986) to 176 days (Simpson and O'Connor 1994). For this test, the duration of the wetting period was 66 days. After this period the rate of moisture accumulation appeared constant, and the wetting trends could be identified. The drying conditions were started. Exterior temperatures used in other experiments have ranged from 7.2°C for mild winter conditions (Zarr et al. 1995) to −18°C for extreme Swedish winter conditions (Ojanen and Simonson 1995). In this case, the exterior temperature for the wetting period corresponds to the coldest part of the year in Montreal. The mean temperature of the last 15 days of December (19°F [−7°C]) and the mean temperature for January (16°F [−9°C]) and February (16°F [−9°C]) are averaged to get an overall outdoor temperature of 17°F (−8.5°C) for the wetting period. The 72°F (22°C) temperature inside the test hut is selected to lie midrange in the winter comfort zone specified in *ANSI/ASHRAE Standard 55-1992, Thermal Environmental Conditions for Human Occupancy*, which lies between 68°F (20°C) and 75°F (24°C). This standard also specifies an indoor relative humidity between 25% and 60% for winter. The relative humidity of 50%, closer to the higher end of the spectrum, is selected because it represents a worse-case scenario and will accentuate the moisture-related problems. A positive air pressure differential of 4 Pa is

created inside the test hut to model a typical stack effect for a Montreal winter climate.

The duration of the drying period was 47 days. The drying conditions were maintained until the moisture contents in the assemblies were stable, the point at which the drying trend could be established. The second half of the month of May is the onset of the drying period in Montreal. Before this time, drying may not occur consistently. The mean temperature of the last 15 days of May (59°F [15°C]) is averaged with the mean temperature of June (65°F [19°C]) to get an overall outdoor average temperature of 63°F (17°C) for a total of 45 days of drying. According to ANSI/ASHRAE Standard 55-1992, the indoor temperature comfort zone for summer is in a higher range than for winter (between 72°F [22°C] and approximately 80°F [27°C]). Since the outdoor conditions for this drying period represent spring and not summer, the indoor temperature of 73°F (23°C) is chosen where winter and summer conditions overlap (between 72°F [22°C] and 75°F [24°C]). Although normally the vapor pressure gradient across exterior wall assemblies naturally varies depending on weather and indoor conditions, in this experiment the same amount of moisture is maintained within the test hut. This reflects the assumptions that the occupants maintain the same rate of moisture generation and that the building is conditioned. From the psychrometric chart, for 73°F (23°C) this translates into a relative humidity of 45%. The pressure differential resulting from the stack effect is reduced to 1 Pa.

AIR LEAKAGE CHARACTERIZATION METHODS

Two-Dimensional Grid Moisture Monitoring

Moisture content monitoring is used to locate potential areas for moisture-related problems within the building envelope. Moisture acts as a marker of the warm moist air exfiltrating through the envelope. As air exfiltrates, some moisture is retained by the hygroscopic materials of the assembly. By studying the moisture contents at different locations, the trajectory of air can be mapped. The results can then be presented in a graphic form by drawing curves of equal moisture contents called "isohygrons."

Moisture contents are monitored extensively, both electronically and manually, using gravimetry. Both methods are used because they measure different characteristics. When sensors are installed, the moisture content at a specific depth in the material is measured. Gravimetry, on the other hand, gives an average moisture content for the whole thickness of the material being monitored. The points monitored for moisture are selected on vertical two-dimensional grids along the anticipated air leakage paths. The grid is tighter at 6 in. (150 mm) around entry and exit points, looser at 24 in. (600 mm) for the rest of the expected path.

Figure 6 shows the installed sensors and gravimetry samples holes before installation of the insulation and of the interior finish. Figure 7 illustrates the moisture monitoring grid for each type of air leakage studied.

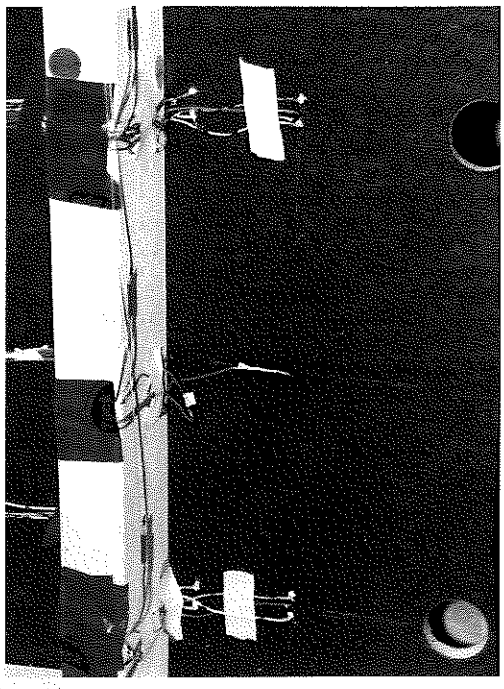

Figure 6 *Photograph of sensors before installation of insulation and finish.*

Electronic Monitoring. Moisture content sensors, consisting of two metal pins, 1/64 in. (1 mm) in diameter by ¼ in. (6 mm) in length, plated with gold to avoid oxidation, are used for the electronic moisture monitoring of the ½ in. (12.5 mm) thick fiberboard sheathing. The resistance of the material to electric current, which is inversely proportional to the moisture content, is measured across the two pins inserted in the material. Readings are taken by applying a voltage to the pins. This voltage ionizes the materials. The ionization is proportional to the number and duration of exposures to the voltage, and it causes corresponding errors in the readings. Because of the long time span of the experiment and the high number of readings required (every 10 minutes for at least 90 days), a custom monitoring system has been developed so that readings of short duration (a few seconds) are taken from each moisture content sensor every 10 minutes. At each reading, the polarity of the pins is reversed, minimizing the error due to the ionization. The moisture content sensors are installed, from inside the test hut, in the fiberboard sheathing to measure the average moisture content of its interior surface layer.

Gravimetry. The test requires continuous moisture monitoring over a long period. To achieve this, gravimetric samples are cut out of the materials to be monitored before the beginning of the test and are used for its complete duration. A customized gravimetric protocol is developed for this experiment to minimize the impact of the sample cutouts on the hygrothermal behavior of the assembly.

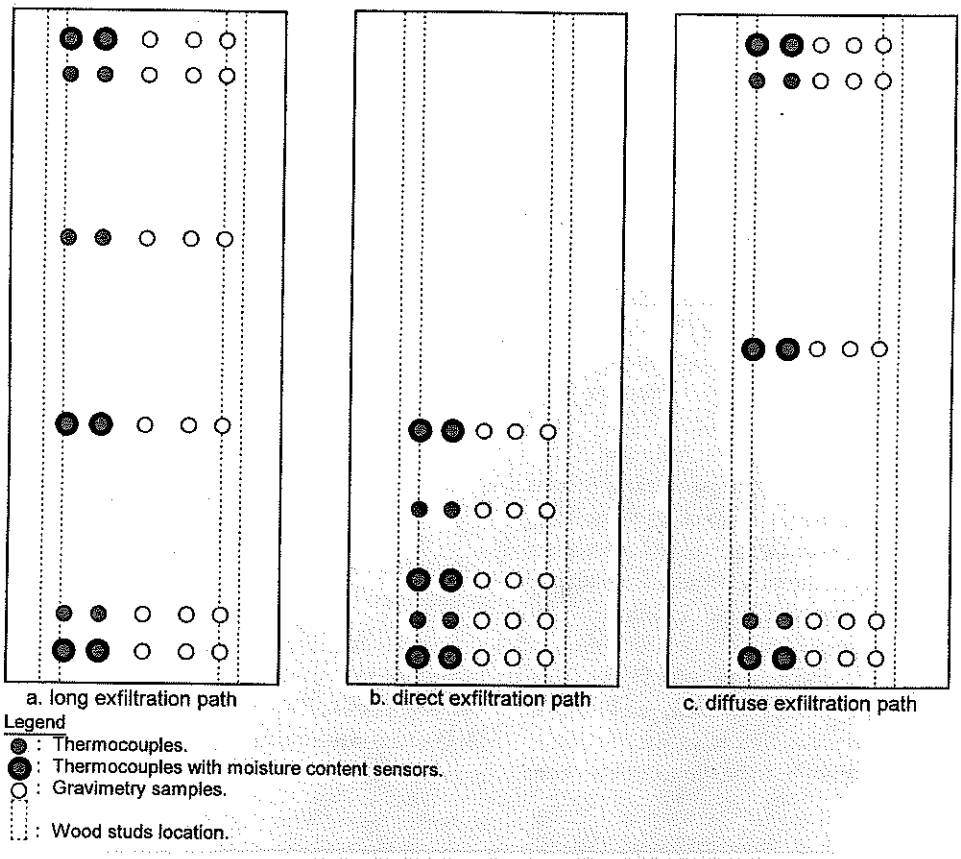

Figure 7 *Moisture content monitoring and thermocouple locations.*

Gravimetric samples are taken on the cold side of the wood studs and in the fiberboard sheathing. The stud samples are ½ in. (12.5 mm) deep by ½ in. (12.5 mm) high by 1½ in. (38 mm) wide. The fiberboard samples are 1½ in. (38 mm) in diameter, except for those in front of the studs, which are 2 in. (50 mm) to give access to the wood stud samples. All are accessible from the outside of the test hut. A photograph of the gravimetric sample holes can be seen in Figure 8.

Holes are cut out of the spunbonded polyolefin membrane, the last material on the cold side of the assemblies, to give access to the samples. This material, commonly used as a wind barrier in residential construction in Quebec, has a very low air permeability and a high water vapor permeability. Between and during weighings, a piece of this membrane sealed with tape is used to cover those holes and impede air leakage through the perimeter of the samples. Because their perimeter cannot be sealed directly, the fiberboard samples must fit tightly enough so that as little air as possible can flow around them, but not so tightly that they cannot be removed without being damaged.

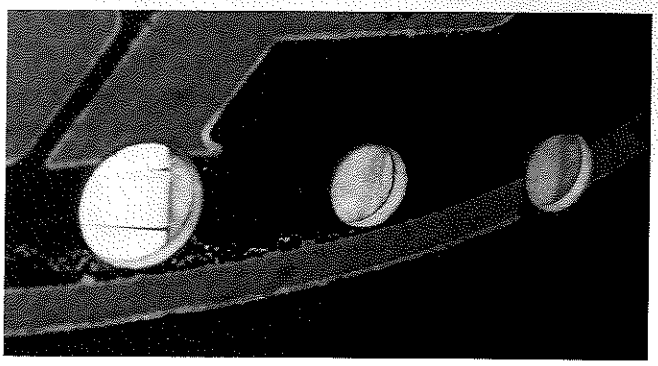

Figure 8 *Gravimetric sample holes.*

During the experiments, all samples are weighed every week for the first 30 days and then every two weeks. Section by section, they are put in sealed plastic bags for handling, weighed on an on-site scale accurate to the microgram, and then put back in their respective positions. The gravimetric sample holes are blocked while the samples are being weighed to avoid airflow through them. The procedure is completed as fast as possible so that the moisture contents of the samples do not have time to vary significantly. At the end of the experiment, the wood samples are oven-dried at 217°F (103°C) according to *ASTM D 4442-92, Standard Test Methods for Direct Moisture Content Measurement of Wood and Wood-Base Materials* (ASTM 1992). The fiberboard samples are dried at 135°F (57°C).

Three-Dimensional Grid Temperature Monitoring

As warm indoor air moves through the assembly, it increases the temperature of the materials with which it comes in contact, thus mapping its own trajectory. This effect is identifiable as long as a sufficient temperature difference exists between outdoor air and indoor air. Hence, this test should confirm the hypothesis that temperatures within an envelope assembly can give indications on the movement of air exfiltrating through it.

Type-T thermocouples (copper and constantan) are placed in the assemblies according to a three-dimensional grid. This grid follows the one used for moisture content monitoring but in two planes instead of one. The locations of the two thermocouple layers within the assemblies are the same for all three insulation strategies: for the outer layer, thermocouples are installed on the interior surface of the fiberboard sheathing, and for the inner layer, they are installed on the interior surface of the fiberglass batt insulation, in line with the thermocouples of the outer layer. Temperature readings are taken every ten minutes for the whole duration of the experiment. Refer to Figure 6 for a photo of a sample section with installed thermocouples before installation of the insulation and the interior finish and to Figure 7 for the location of the thermocouples.

By measuring temperatures in such a way, temperature maps at two different planes within the building envelope are produced. From these maps, a pattern for air exfiltration may be extrapolated.

RESULTS AND DISCUSSION

The test is completed, but gravimetry moisture content results are still being analyzed. Calibration of the electronic moisture content sensors is underway.

However, the temperature monitoring results can be readily presented. The temperatures used to generate Figures 9 and 10 are the averages of all the readings for each monitoring point for the second week of testing, when temperature equilibrium had been reached. By then, nonsignificant moisture buildup had occurred in the assemblies. For the discussion, the temperatures at the warm surface of the fiberglass batt insulation will be referred to as "warm plane" temperatures and those at the cold surface of the fiberglass batt insulation as "cold plane" temperatures.

Figure 9 presents the temperature gradients across the studs and the insulation at three different heights for three sample sections with no rigid insulation added. This representation allows comparison of monitored temperature gradients at different heights for different air leakage patterns and highlights the effect of the thermal bridges caused by the wood studs.

The temperature gradients are more important through the insulation than across the wood studs. At the 3 ft (900 mm) and 6 ft, 11 in. (2100 mm) levels, the temperatures are higher in both planes for the long leakage path than for the direct leakage path and the airtight section, indicating that the air is warming the materials as it flows up. At the 12 in. (300 mm) level, which is the height of the direct leakage opening, higher temperatures are found in the direct path wall. The difference in temperature gradients between the different air leakage paths is more pronounced across the studs. This may be due to air exfiltrating along the studs. However, before the installation of the interior finish, the construction was checked to ensure that there was no gap between the studs and the fiberglass batt insulation.

Figure 10 presents the temperature maps for these sections. Figures 10a and 10d show the temperature curves for the cavity with no added rigid insulation and no air leakage on the warm and cold planes, respectively. It can be seen that the isotherms on the warm plane are parallel, indicating that the vertical temperature gradient is small. The pattern produced is analogous to that of conductive heat transfer without the influence of convective heat transfer.

The temperature maps on the warm plane for the long air exfiltration path (Figure 10b) show the tendency to be warmer in the upper half of the cavity, as if the materials are warmed by the exfiltration air as it flows up. This is apparently not due

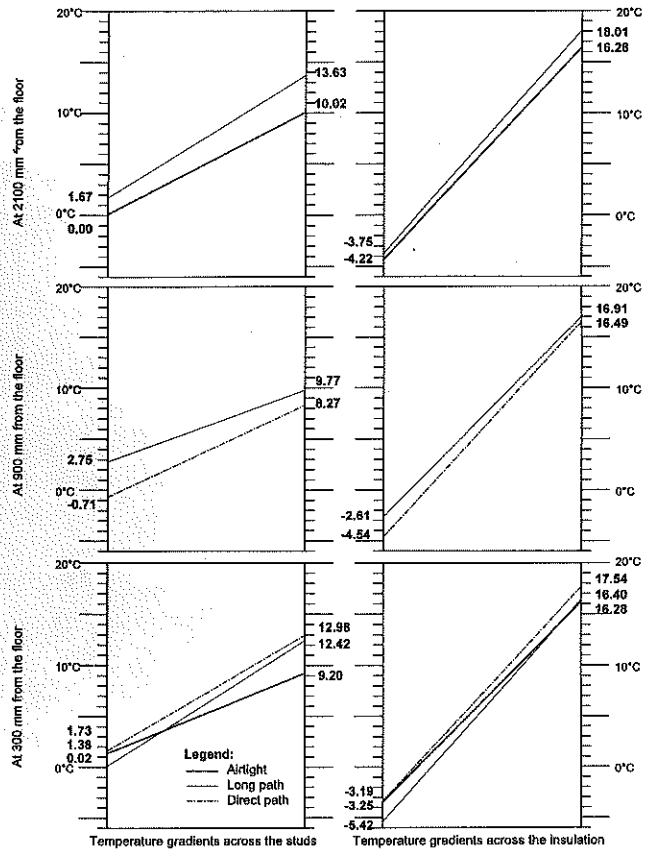

Figure 9 *Temperature gradients across the studs and across the insulation for three base-case assemblies.*

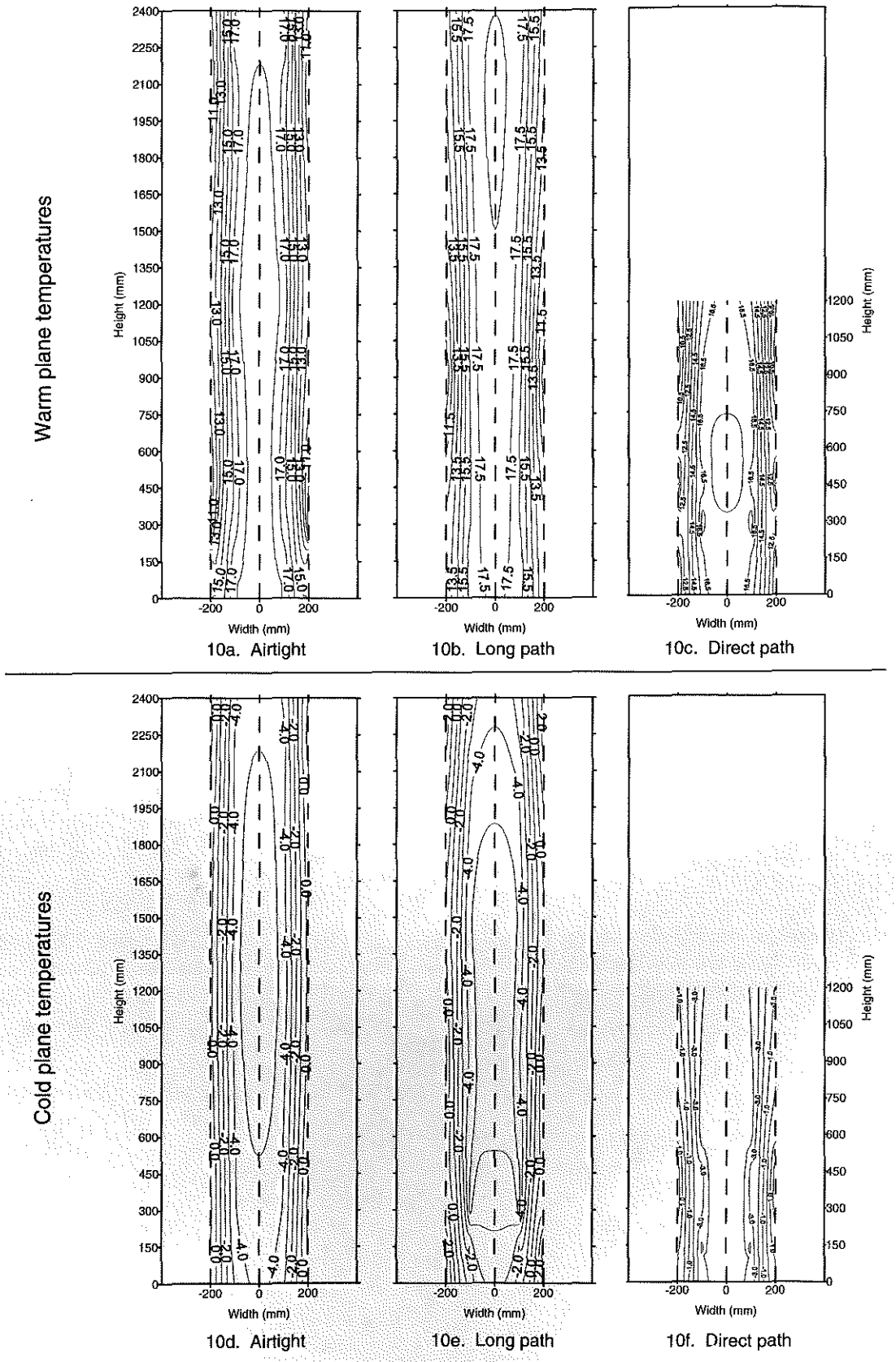

Figure 10 *Warm and cold plane isotherms for three base-case assemblies.*

to temperature stratification in the test hut, as the air is well mixed and has a maximum 1.8°F (1°C) average temperature difference from floor to ceiling, but depends on air leakage. On the cold plane (Figure 10e), the temperatures are warmer at the bottom, opposite the air entry point.

The temperature maps on the warm plane for the cavity with the direct air exfiltration path (Figure 10c) show warmer temperatures around the location of the opening in the interior finish, in the lower part of the sample sections where the warm indoor air flows into the cavity. For those cavities, the temperatures on the cold plane are coldest around the location of the hole (Figures 10f), directly opposite the warmer temperatures measured on the warm side of the insulation.

CONCLUSION

A full-scale wood frame test hut was built inside an environmental chamber. This test hut was subjected to 66 days of simulated winter and then to 47 days of late spring weather conditions. The assemblies tested were insulated according to three different strategies and had different air leakage characteristics. Temperatures were monitored according to a three-dimensional grid at two different planes within the assemblies, and moisture contents were monitored according to a two-dimensional grid in an attempt to map the movement of exfiltrating air. The resulting temperature gradients (Figure 9) and isotherms (Figure 10) are presented. These results show a correlation between temperature profiles and air leakage patterns. This relationship may form the basis for the development and improvement of modeling moisture migration.

ACKNOWLEDGMENTS

Special thanks for the technical and engineering support of Dr. Jiwu Rao, research engineer, and Mr. Luc Demers, electronic instrument technician.

This research is partly supported by the External Research Program of the Canada Mortgage and Housing Corporation.

REFERENCES

ASTM. 1989. ASTM C 236-89, Standard test method for steady-state thermal performance of building assemblies by means of a guarded hot box. *Annual Book of Standards*, Vol. 04.06, pp. 52-62. American Society for Testing and Materials.

ASTM. 1992. ASTM D 4442-92, Standard test method for direct measurement of wood and wood-based materials. *Annual Book of Standards*, Vol. 04.10, pp. 493-497. American Society for Testing and Materials.

Fazio, P., D. Derome, D. Gerbasi, A. Athienitis, S. Depani, and P. Kovacevic. 1998. Testing of flat roofs insulated with cellulose fiber. *Thermal Performance of the Exterior Envelopes of Buildings VII.* Atlanta: American Society of Heating, Refrigerating and Air-Conditioning Engineers, Inc.

Fazio, P., A. Athienitis, C. Marsh, and J. Rao. 1997. An environmental chamber for investigation of building envelope performance. *Journal of Architectural Engineering*, Vol. 3, No. 2, pp. 97-102. American Society of Civil Engineers.

Forest, T. 1989. Moisture transfer through walls. *Thermal Performance of the exterior envelopes of Buildings IV,* pp. 532-542. Atlanta: American Society of Heating, Refrigerating and Air-Conditioning Engineers, Inc.

Kumaran, M.K. 1996. Taking guess work out of placing air/vapor barriers. *Canadian Consulting Engineer.* March/April, pp. 32-33.

Ojanen, T., and R.O. Kohonen. 1995. Hygrothermal performance analysis of wind barrier structures. *ASHRAE Transactions* 101(1): 595-606.

Ojanen, T., and C. Simonson. 1995. Convective moisture accumulation in structures with additional inside insulation. *Thermal Performance of the Exterior Envelopes of Buildings VI,* pp. 745-752. Atlanta: American Society of Heating, Refrigerating and Air-Conditioning Engineers, Inc.

Simpson, A., and D.E. O'Connor. 1994. Timber frame wall: Hygrothermal properties and vapour barrier damage. *Building Services Engineering Research and Technology,* Vol. 15, No. 3. pp. 179-184.

Trechsel, H.R., P.R. Achenbach, and J.R. Ebbets. 1985. Effect of an exterior air infiltration barrier on moisture accumulation within insulated frame wall cavities. *ASHRAE Technical Data Bulletin*, Vol. 1, No. 2, pp. 23-37.

Trechsel, H.R., P.R. Achenbach, H.J. Knight, and G.W. Lou. 1986. Evaluation of wind effect on moisture content of frame walls with and without an air-infiltration barrier. *Thermal Performance of the Exterior Envelopes of Buildings III,* pp. 648-662. Atlanta: American Society of Heating, Refrigerating and Air-Conditioning Engineers, Inc.

Zarr, R.R., D.M. Burch, and A.H. Fanney. 1995. Heat and moisture transfer in wood-based wall construction: Measured versus predicted. *NIST Building Science Series 173.* Building and Fire Research Laboratory, National Institute of Standards and Technology. Gaithersburg, MD. 72 p.